

High-performance variants of plant diacylglycerol acyltransferase 1 generated by directed evolution provide insights into structure function

Guanqun Chen^{1,*}, Yang Xu¹, Rodrigo M. P. Siloto¹, Kristian Mark P. Caldo¹, Thomas Vanhercke², Anna El Tahchy², Nathalie Niesner², Yongyan Chen¹, Elzbieta Mietkiewska¹ and Randall J. Weselake^{1,*}

¹Department of Agricultural, Food and Nutritional Science, University of Alberta, Edmonton Alberta, Canada, T6G 2P5, and ²CSIRO Agriculture & Food, Canberra, ACT, Australia

Received 23 May 2017; revised 27 June 2017; accepted 24 July 2017.

*For correspondence (e-mails randall.weselake@ualberta.ca; guanqun.chen@ualberta.ca).

SUMMARY

Diacylglycerol acyltransferase 1 (DGAT1) catalyzes the acyl-CoA-dependent biosynthesis of triacylglycerol, the predominant component of seed oil. In some oil crops, including *Brassica napus*, the level of DGAT1 activity can have a substantial effect on triacylglycerol production. Structure–function insights into DGAT1, however, remain limited because of the lack of a three-dimensional detailed structure for this membrane-bound enzyme. In this study, the amino acid residues governing *B. napus* DGAT1 (BnaDGAT1) activity were investigated via directed evolution, targeted mutagenesis, *in vitro* enzymatic assay, topological analysis, and transient expression of cDNA encoding selected enzyme variants in *Nicotiana benthamiana*. Directed evolution revealed that numerous amino acid residues were associated with increased BnaDGAT1 activity, and 67% of these residues were conserved among plant DGAT1s. The identified amino acid residue substitution sites occur throughout the BnaDGAT1 polypeptide, with 89% of the substitutions located outside the putative substrate binding or active sites. In addition, cDNAs encoding variants I447F or L441P were transiently overexpressed in *N. benthamiana* leaves, resulting in 33.2 or 70.5% higher triacylglycerol content, respectively, compared with native BnaDGAT1. Overall, the results provide novel insights into amino acid residues underlying plant DGAT1 function and performance-enhanced BnaDGAT1 variants for increasing vegetable oil production.

Keywords: triacylglycerol biosynthesis, diacylglycerol acyltransferase, directed evolution, topology, leaf oil production, *Brassica napus*, *Nicotiana benthamiana*.

INTRODUCTION

Plant oils are mainly composed of the storage lipid triacylglycerol (TAG) (Weselake, 2005). In developing seeds of oleaginous crops, such as oilseed rape (*Brassica napus* and *Brassica rapa*) and soybean (*Glycine max*), seed TAG serves as an energy depot supporting germination and early seedling growth. Storage lipids are also necessary constituents of food and animal feed, and can serve as a substitute for dwindling petrochemical reserves in the form of renewable feedstock for the production of biodiesel and industrial chemicals (Carlsson *et al.*, 2011). With the limited availability of arable land and our ever-increasing population, it is of paramount importance to generate oleaginous crops with increased oil productivity, both in seed and non-seed tissues (Carlsson *et al.*, 2011; Weselake, 2016).

Plant TAG biosynthesis involves the action of acyl-CoA-dependent and acyl-CoA-independent acyltransferases (Chen *et al.*, 2015). In the traditional acyl-CoA-dependent *sn*-glycerol-3-phosphate pathway, also known as the Kennedy pathway, three acyltransferases, namely *sn*-glycerol-3-phosphate acyltransferase, lysophosphatidic acid acyltransferase and diacylglycerol acyltransferase (DGAT; EC 2.3.1.20), catalyze the sequential acylation of the *sn*-1, *sn*-2 and *sn*-3 positions, respectively, of the glycerol backbone. DGAT catalyzes the final step in TAG biosynthesis, using *sn*-1,2-diacylglycerol and acyl-CoA as substrates (Liu *et al.*, 2012). DGAT activity resides in at least two distinct membrane-bound polypeptides, referred to as DGAT1 and DGAT2. The overexpression of cDNAs encoding plant DGAT1 has been used to increase seed oil deposition in

Arabidopsis thaliana and oil crops such as soybean and oilseed rape (Jako *et al.*, 2001; Weselake *et al.*, 2008; Roesler *et al.*, 2016). These results highlighted the value of DGAT1 as a biotechnological tool for increasing seed oil content. Moreover, plant DGAT1 has also been used to increase TAG content in non-seed biomass and oleaginous microorganisms (Greer *et al.*, 2015; Vanhercke *et al.*, 2017). To explore the full potential of DGAT in TAG biosynthesis, it is imperative to gain insight into the enzyme's mechanism of activity. As DGAT1 is an integral membrane protein with multiple transmembrane domains (TMDs), its three-dimensional structure and the ensuing experiments that would shed light on structure–function relationships in the enzyme are yet to be described (Liu *et al.*, 2012; Lopes *et al.*, 2014, 2015).

One possible approach to gain insight into structural aspects underlying enzyme action in the absence of a detailed three-dimensional structure is to generate enzyme variants with amino acid residue substitutions affecting enzyme activity (Cheng *et al.*, 2015). Enzyme variants can be generated by various methods, including site-directed mutagenesis and directed evolution. Single amino acid residue substitutions resulting in increased DGAT activity have previously been identified in maize (*Zea mays*) DGAT1 (Zheng *et al.*, 2008) and bovine DGAT1 (Grisart *et al.*, 2002; Winter *et al.*, 2002). Directed evolution is a powerful tool for protein engineering (Packer and Liu, 2015) that has been used to generate DGAT1 variants with enhanced activity (Siloto *et al.*, 2009a; Roesler *et al.*, 2016). Previously, we developed a library of *B. napus* DGAT1 (BnaDGAT1) variants and established a yeast-based high-throughput screening method to screen for BnaDGAT1 mutants with modified activity (Siloto *et al.*, 2009a,b). As *B. napus* is an important oil crop in the Brassicaceae family and closely related to the model plant *Arabidopsis*, exploring structure function in BnaDGAT1 would be valuable for both basic plant lipid biology and metabolic engineering of seed oil production. In addition, high-biomass crops, including tobacco (e.g. *Nicotiana tabacum*) and sugarcane (*Saccharum officinarum*), have attracted significant attention as alternative platforms for lipid production for food, biofuel and industrial feedstock (Zale *et al.*, 2016; Vanhercke *et al.*, 2017). As DGAT1 overexpression can increase TAG levels in non-seed tissues (Vanhercke *et al.*, 2013; Zale *et al.*, 2016), it would be useful to determine whether the BnaDGAT1 variants generated via directed evolution can further increase lipid content in *Nicotiana benthamiana* leaves, compared with the native BnaDGAT1. In this study, we explored the possible function of amino acid residues affecting BnaDGAT1 performance through directed evolution, targeted mutagenesis, *in vitro* enzymatic assay and topological analysis. In addition, we evaluated the application of performance-enhanced DGAT1 variants in increasing TAG production using an *N. benthamiana* transient

expression system. Results from this study provide insight into structure function in plant DGAT1, which has the potential to be harnessed for the improvement of vegetable oil production in seeds, vegetative tissues and microorganisms.

RESULTS

Identification of amino acid residue substitutions affecting BnaDGAT1 activity

Developing insight into amino acid residues affecting BnaDGAT1 activity may be useful in probing structure function in this enzyme. In our previous work, three libraries of *BnaDGAT1* variants were created by error-prone PCR (Siloto *et al.*, 2009a). The current study focused on 50 of the recombinant performance-enhanced BnaDGAT1 variants identified via directed evolution (Figure 1; Table S1). TAG content and fatty acid composition of the TAG of 50 *Saccharomyces cerevisiae* H1246 strains hosting the BnaDGAT1 variants were further analyzed by GC/MS. H1246 is a quadruple mutant devoid of TAG synthesis, therefore any new TAG production is dependent on the introduction of cDNA encoding a functional DGAT (Sandager *et al.*, 2002). All of the BnaDGAT1 variants resulted in higher TAG content when produced in yeast (Figure 1), but had almost no influence on the fatty acid compositions of the TAG (Table S2).

The cDNAs encoding the 50 BnaDGAT1 variants were sequenced to identify the positions of amino acid residue substitutions. A total of 104 amino acid residue substitutions at 81 sites were identified (Figure S1; Table S1). Analysis of 22 plant DGAT1s indicated that the majority of the 81 modification sites (67%) are conserved among different plant species (Figure S2; Table S3). As many of the 50 BnaDGAT1 variants contained multiple mutations, it was necessary to generate single amino acid residue changes to further explore how individual substitutions affected DGAT1 activity. Twenty-seven amino acid residue substitutions at 26 amino acid sites were selected to generate single-site mutants, which were individually expressed in yeast H1246 for further analysis (Figure S1, underlined). In yeast cells harvested at the early stationary phase, 19 and six single-site mutants resulted in higher and lower neutral lipid contents, respectively, based on the results of the Nile red assay (Figure 2, $P < 0.05$). These amino acid substitutions were used to study structure–function relationships in BnaDGAT1 activity.

Characterization of BnaDGAT1 variants with single amino acid residue substitutions

Four performance-enhanced BnaDGAT1 variants with single amino acid residue substitutions (S112R, F302C, L441P and I447F) and one variant (I287V) resulting in a lower level of TAG were selected for detailed characterization. S112R

Figure 1. Triacylglycerol (TAG) content of yeast strains producing BnaDGAT1 variants. TAG contents (mean \pm SDs) of the yeast H1246 cells were analyzed by GC/MS. Vectors hosting mutagenized *BnaDGAT1s*, *LacZ* gene (negative control 1, VEC) and wild-type (WT) *BnaDGAT1* (negative control 2, WT) were expressed in a quadruple mutant *Saccharomyces cerevisiae* strain H1246, which is devoid of TAG synthesis (Sandager *et al.*, 2002). Statistical analysis was performed using one-way ANOVA. The TAG contents of all mutants were significantly higher than in the WT ($P < 0.01$).

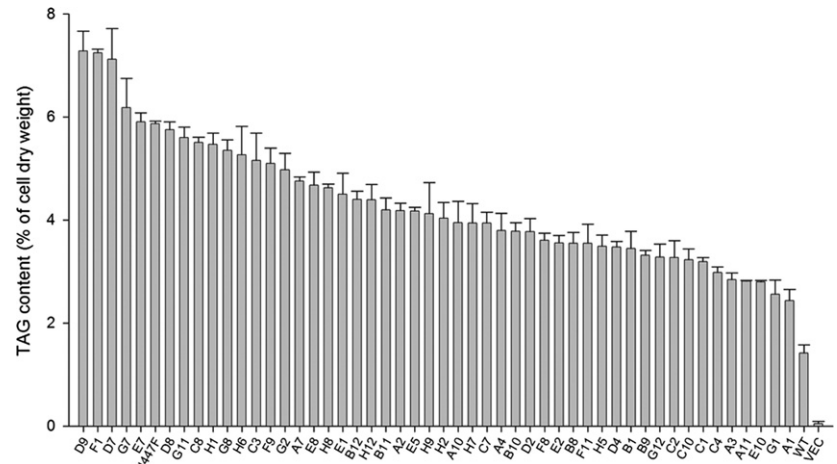
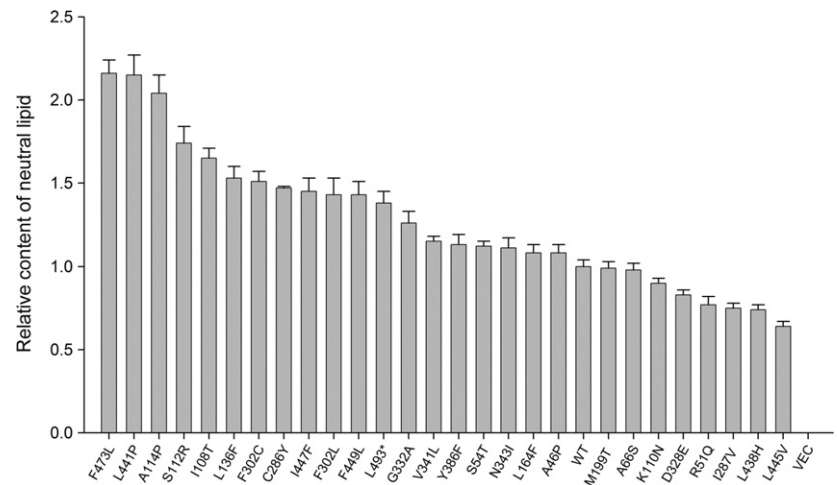


Figure 2. Relative neutral lipid content of yeast H1246 strains hosting BnaDGAT1 variants generated by single-site mutagenesis. Mutagenized *BnaDGAT1s*, *LacZ* gene (negative control 1, VEC) and wild-type (WT) *BnaDGAT1* (negative control 2, WT) were expressed into a quadruple mutant *Saccharomyces cerevisiae* strain H1246, which is devoid of triacylglycerol synthesis. Neutral lipid contents of the yeast cells were analyzed with the Nile red fluorescence assay and presented as fold-increase compared with the WT control (the value of the WT was set as 1). Oil contents of all variants, except M199T and A66S, significantly different from that of the WT (one-way ANOVA, $P < 0.05$). *Stop codon.



and L441P grew slower than the wild type (WT), whereas the other three showed similar growth rates to the WT (Figure S3a). The yeast line producing native BnaDGAT1 and all lines producing enzyme variants exhibited high transcript and protein levels at all measured time points up to the stationary phase (Figure S3b–d). Yeast producing variants S112R, F302C, L441P or I447F had higher neutral lipid content than yeast producing native BnaDGAT1 at all time points, whereas variant I287V had a lower TAG content (Figure 3a). In general, BnaDGAT1 variants resulting in higher yeast neutral lipid content exhibited a higher microsomal enzyme-specific activity than for microsomes from yeast producing native BnaDGAT1 (Figure 3b). Variant I287V, however, showed lower enzyme-specific activity compared with native BnaDGAT1 (Figure 3b). In addition, yeast cells were also harvested at early stationary phase for determination of TAG content and fatty acid composition of TAG by GC/MS. The TAG contents of the yeast strains (Figure 3c) were consistent with Nile red assay results (Figure 3a), whereas all yeast lines, producing the

native BnaDGAT1 or different variants, had TAGs with similar fatty acid compositions (Figure 3c), which indicated that the amino acid residue substitutions mainly affected TAG content and not the fatty acid composition of TAG.

To further analyze the effect of amino acid residue substitutions of BnaDGAT1 on storage lipid biosynthesis, site saturation mutagenesis was performed at site 447, where the substitution of I with F resulted in a substantial increase in the neutral lipid content of the yeast (Figure 2). The *BnaDGAT1* mutants were then expressed in yeast SCY62 (wild type) or H1246 strains, and yeast cells were harvested at early stationary phase for analysis of neutral lipid content. As shown in Figure 4, several amino acid residue substitutions for I were effective in substantially increasing the neutral lipid content of the wild type or yeast H1246. The replacement of I with A, C, F, L, T or V resulted in substantially higher neutral lipid content, whereas the replacement of I with D, E, N, R, K, Y or the stop codon (*) resulted in substantially lower neutral lipid content. As I, A, C, F, L and V are hydrophobic amino acid residues, whereas D, E, N, R

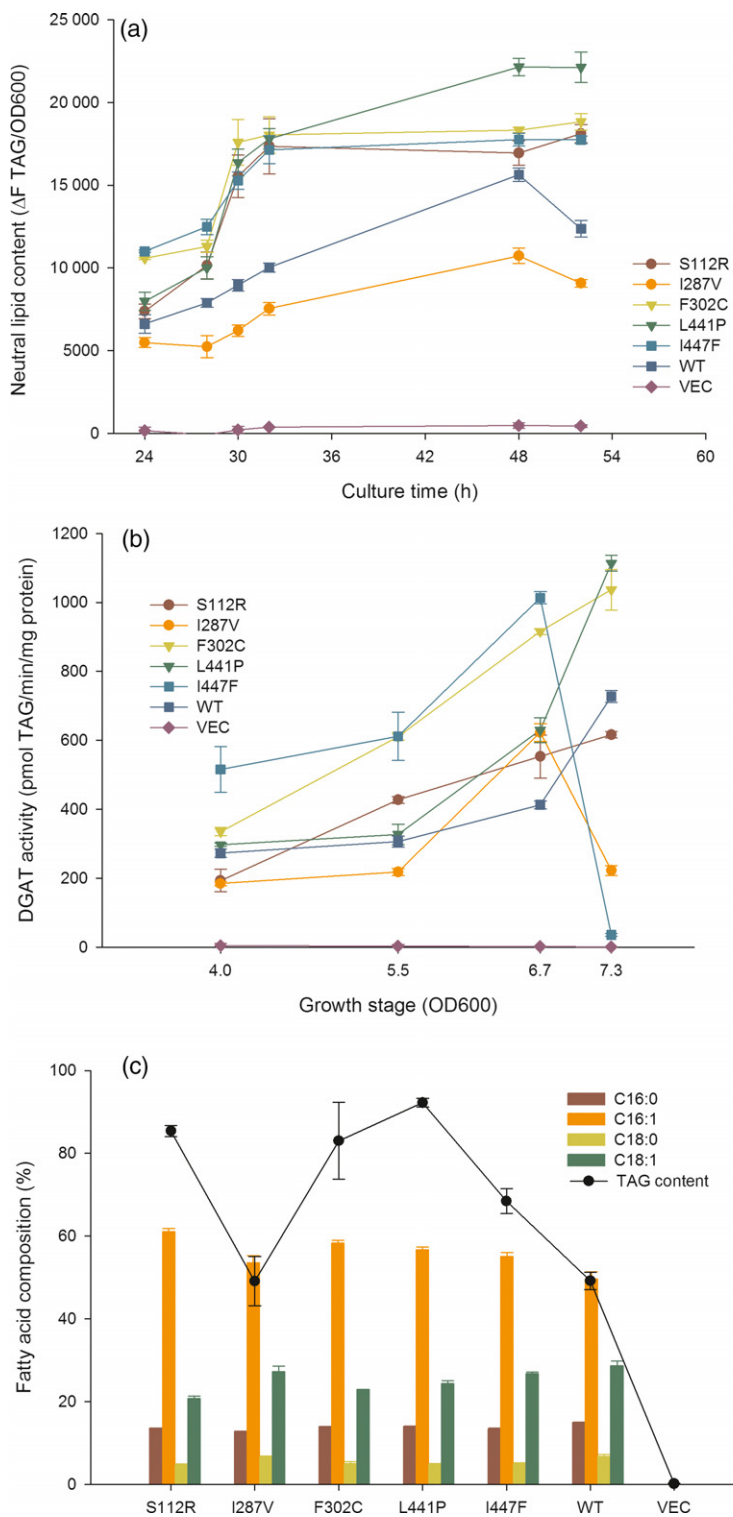


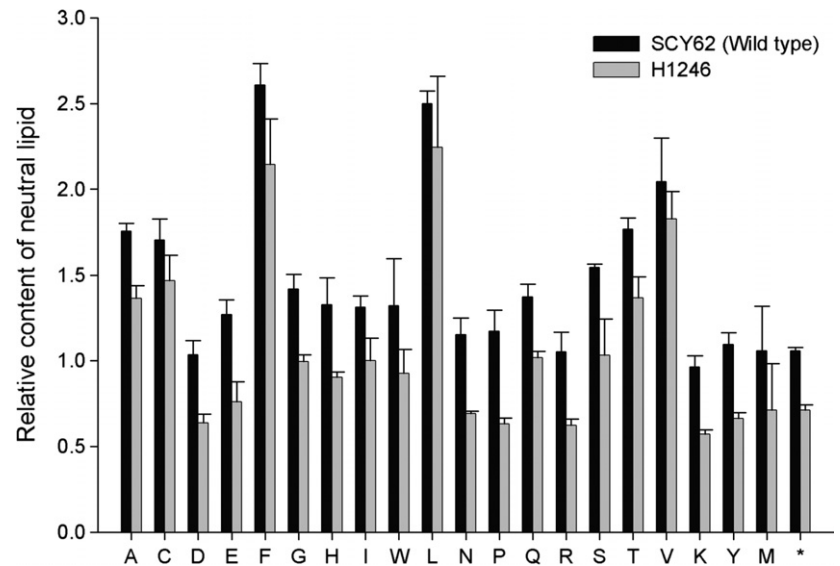
Figure 3. Characterization of five selected BnaDGAT1 single-site mutants: S112R, I287V, F302C, L441P and I447F. (a) Neutral lipid content of yeast strains. (b) DGAT1 activity of the selected variants. (c) Triacylglycerol (TAG) content and fatty acid composition of TAG yeast strains, measured by GC/MS. Vectors hosting mutagenized *BnaDGAT1s*, *LacZ* gene (negative control 1, VEC) and wild-type (WT) *BnaDGAT1* (negative control 2, WT) were expressed into a quadruple mutant *Saccharomyces cerevisiae* strain H1246, which is devoid of TAG synthesis.

and K are all polar, the results indicated that substitution of I with a more polar amino acid residue at site 447 might lead to a decrease in DGAT activity. Substitution of I with T or Y were exceptions to this.

Amino acid residue substitutions affecting BnaDGAT1 activity in relation to enzyme topology

For a more comprehensive analysis of the effect of amino acid residue substitution on BnaDGAT1 activity, all the

Figure 4. Relative neutral lipid content of the site saturation mutagenesis BnaDGAT1 variants at position 447. Vectors hosting mutagenized *BnaDGAT1s*, *LacZ* gene (negative control 1, VEC) and wild-type *BnaDGAT1* (negative control 2, WT) were expressed in quadruple mutant *Saccharomyces cerevisiae* strain H1246, which is devoid of triacylglycerol synthesis, and its parental strain SCY62, respectively (Sandager *et al.*, 2002). Neutral lipid contents of the yeast cells were analyzed with the Nile red fluorescence assay (Siloto *et al.*, 2009b) and presented as fold-changes from the H1246 strain hosting native BnaDGAT1 (I447, the value was set as 1). *Stop codon.



mutation sites identified via directed evolution were labeled on a predicted BnaDGAT1 topology model (Figure 5). Although the amino acid residue substitution sites occurred throughout the BnaDGAT1 primary structure (Figure S1), topological analysis revealed certain patterns. Among the 81 sites of amino acid residue substitution (Figure 5, blue circles), 24 sites (30%) were localized within the hydrophilic region (residues 1–100) at the N-terminus, away from the first predicted TMD. Nine (residues 437–458) and five (residues 473–493) sites were identified within or close to the ninth and 10th TMDs at the C-terminus, accounting for 38 and 23% of the amino acid residues of the TMDs, respectively. The functional importance of the C-terminus of DGAT1 relates to results of the site saturation mutagenesis experiment at site 447 (Figure 4). As site 447 is buried in a TMD, the change of hydrophobic amino acid residue to a more polar residue might have structural effects associated with altered enzyme activity (Figures 4 and 5). It may also be energetically unfavorable to have a polar residue buried within the bilayer.

Among the 19 variants with single amino acid residue substitutions that resulted in higher TAG accumulation (Figure 2), 15 amino acid residue sites are either within or close to a TMD; exceptions are A46P at the N-terminus, C286Y on the loop between the fifth and the sixth TMD, G332A on the loop between the sixth and the seventh TMD, and Y386F on the loop between the seventh and the eighth TMD. Moreover, 15 amino acid residue substitution sites, including A46P, I108T, A114P, L136F, L164F, F302C, F302L, G332A, V341L, Y386F, L441P, I447F, F449L, F473L and L493* correspond to nonpolar amino acids. All the amino acid residues except L493* and I108T were substituted by amino acid residues of similar polarity, which

may contribute to a more suitable enzyme conformation in support of catalysis. The remaining three single site variants (S54T, S112R and N343I) have substitutions with polar amino acid residues. Among them, S54 and S112 are substituted with amino acid residues with similar polarities, whereas N343 is substituted with a nonpolar amino acid residue. As N343 is located close to the seventh TMD, the substitution of a polar N with a nonpolar I might encourage this amino acid residue to be buried in the membrane.

It was proposed that the region just preceding the predicted TMD1 (putative acyl-CoA binding site 1), which is the most conserved region of the N-terminus, might be a putative acyl-CoA binding site (Jako *et al.*, 2001; Nykiforuk *et al.*, 2002). Another proposed acyl-CoA binding site (putative acyl-CoA binding site 2) includes the motif FYXDWWN, which is largely conserved among DGATs and acylcholesterol acyltransferases (Lopes *et al.*, 2014, 2015). A synthetic peptide of the FYXDWWN motif was used to analyze its interaction with acyl-CoA substrate and observed that this region appears to bind the acyl chain of the substrate. In the same study, they also demonstrated the interaction of DAG with the putative DAG binding site HXXXXRHXXXP (Lopes *et al.*, 2014). This motif is also present in protein kinase C and diacylglycerol kinase. Several amino acid residue substitutions in the variants are within the putative acyl-CoA binding site in the N-terminal region or the putative active site 2 or 3, but there are no amino acid residue substitutions within the putative DAG binding site (Figure 5). Four single-site variants (I108T, K110N, S112R and A114P) have amino acid residue substitutions located in the putative acyl-CoA binding site, with three of them resulting in higher neutral lipid content in yeast (Figure 2), indicating that this site may play an important role in the activity of DGAT. The single amino acid residue

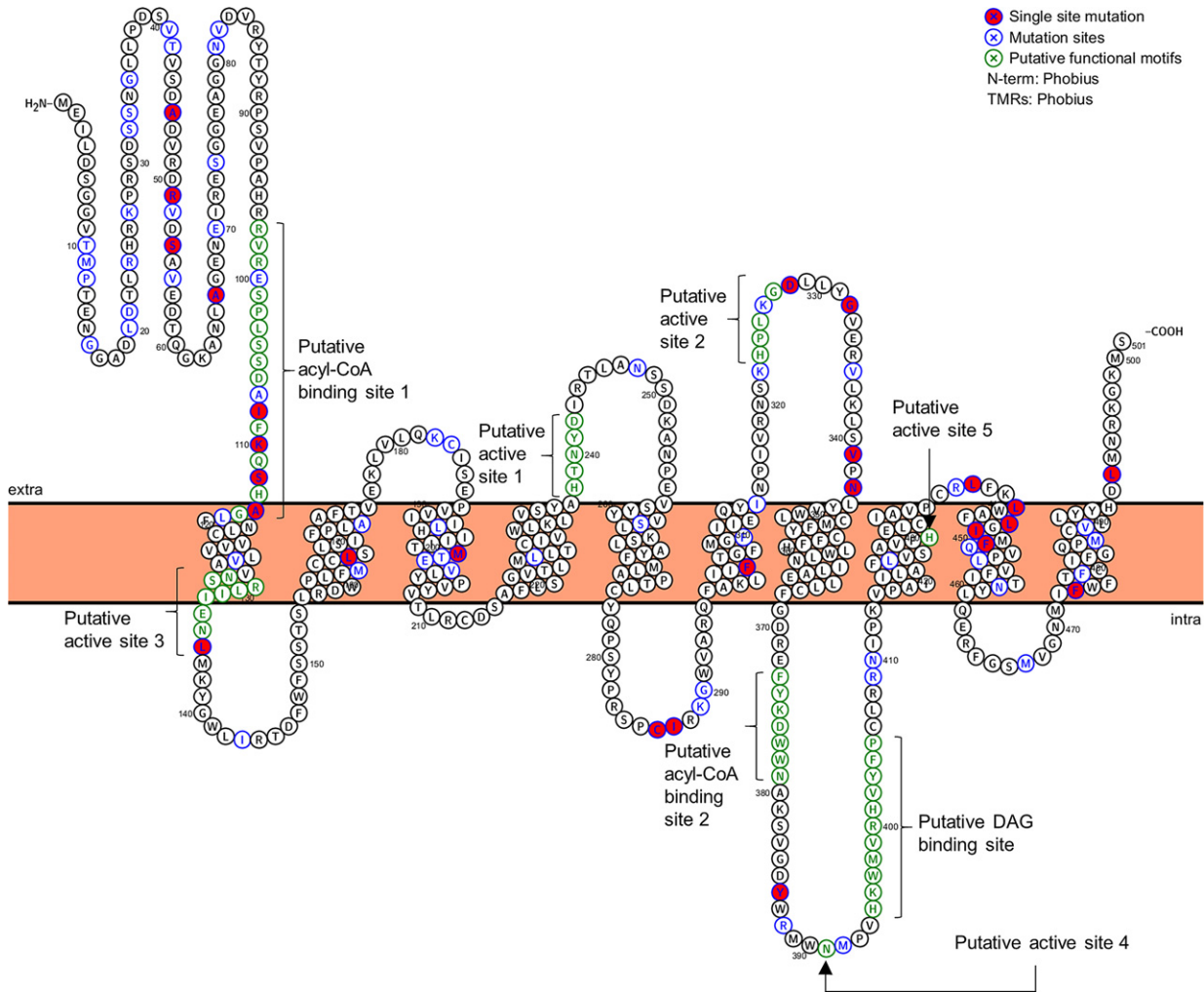


Figure 5. The positions of the identified amino acid residue sites on the predicted topology model of BnaDGAT1. The membrane topology of BnaDGAT1 was predicted by Protter (Omasits *et al.*, 2014). The original amino acid sequence of BnaDGAT1 is represented by black circles. The putative functional sites are presented by green circles. The amino acid modifications selected by directed evolution are represented by blue circles. The single site modifications are represented by blue circles filled with red.

substitution within putative active site 3 (L136F) also contributed to increased yeast lipid accumulation.

High-performance BnaDGAT1 variants increase triacylglycerol accumulation in *N. benthamiana* leaves

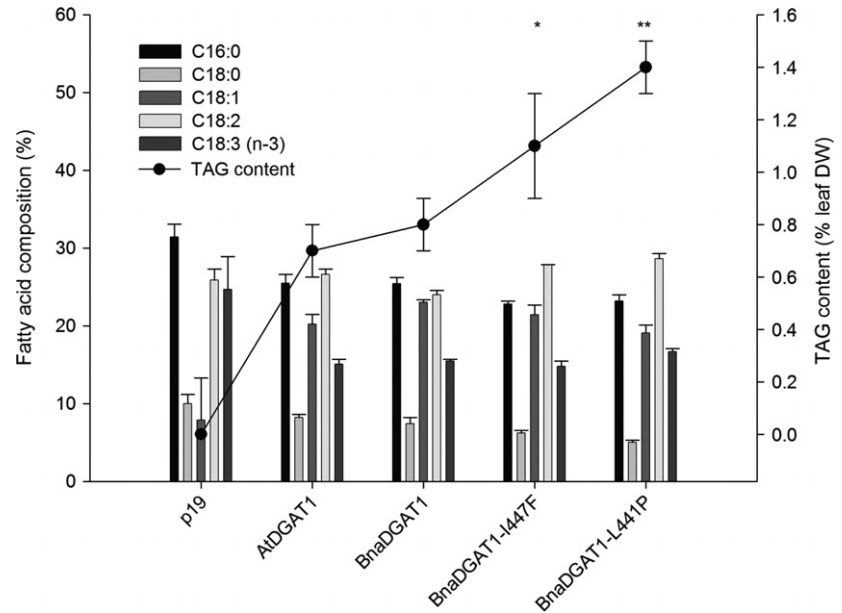
Previous studies indicated that the co-expression of cDNAs encoding *A. thaliana* DGAT1 (*AtDGAT1*) and *WRINKLED1* (*AtWRI1*) results in a substantial increase of TAG accumulation in *N. benthamiana* leaves (Vanhercke *et al.*, 2013). In order to determine whether BnaDGAT1 variants can result in higher leaf TAG than the native enzyme, cDNAs encoding two variants showing high activity in yeast (I447F and L441P) were co-expressed individually with *AtWRI1* in the *N. benthamiana* transient expression system. The effect of expressing cDNA encoding native Arabidopsis DGAT1 is shown for comparative purposes. As shown in Figure 6,

the overexpression of cDNAs encoding BnaDGAT1-I447F or BnaDGAT1-L441P led to 33.2% ($P < 0.05$) or 70.5% ($P < 0.01$) higher TAG content, respectively, compared with the expression of native *BnaDGAT1* cDNA. In each case, the fatty acid composition of TAG was similar. The results indicated that the BnaDGAT1 variants could be used to increase TAG content in leaf tissues without affecting the fatty acid composition. Taken together, single amino acid residue substitutions identified via directed evolution outside predicted active sites could enhance DGAT1 activity and be used to increase TAG content in vegetative tissue.

DISCUSSION

Various studies have shown that the overexpression of *DGAT1* can increase oil content in plants, microorganisms or animals (Jako *et al.*, 2001; Weselake *et al.*, 2008; Xu

Figure 6. Triacylglycerol (TAG, % of tissue dry weight) and fatty acid composition in transiently transformed *Nicotiana benthamiana* leaf tissue. All cDNAs were constitutively expressed by the CaMV 35S promoter with the co-expression of tomato (*Solanum lycopersicum*) bushy stunt virus p19 viral silencing suppressor gene (p19) and with *Arabidopsis thaliana* WRINKLED1 (*AtWRI1*), except for the negative control p19 where no *WRI1* or *DGAT1* genes were co-expressed. AtDGAT1, P19 + *AtWRI* + *A. thaliana* DGAT1 (*AtDGAT1*); BnaDGAT1, P19 + *AtWRI* + *Brassica napus* native BnaDGAT1; BnaDGAT1-I447F, P19 + *AtWRI* + BnaDGAT1-I447F; BnaDGAT1-L441P, P19 + *AtWRI* + BnaDGAT1-L441P. Error bars denote standard deviations, with $n = 6$ for all samples. Asterisks indicate oil content that significantly differs from the oil content of native BnaDGAT1: * $P < 0.05$; ** $P < 0.01$. Statistical analysis was performed using the Student's *t*-test.



et al., 2008; Greer *et al.*, 2015; Roesler *et al.*, 2016). In contrast, comparatively little is known about structure–function relationships in plant DGAT1 because of the absence of a three-dimensional structure for this membrane-bound enzyme. Enzyme variants produced through directed evolution, however, can be useful for gaining insights into structure function in the absence of a three-dimensional structure (Cheng *et al.*, 2015; Packer and Liu, 2015). In the current study, random mutagenesis using error-prone PCR was used to develop a collection of *BnaDGAT1* cDNAs that encoded recombinant enzyme variants with higher or lower activity than the native enzyme. BnaDGAT1 variants with amino acid residue substitutions were evaluated based on their ability to catalyze the formation of TAG in a yeast strain devoid of TAG synthesis. One hundred and four amino acid residue substitutions were identified at 81 sites in BnaDGAT1, and 32 of the 50 BnaDGAT1 variants (64%) had multiple amino acid residue substitutions (Figures 1, 6 and S2; Table S1).

To further elucidate the contribution of individual amino acid residue substitutions to DGAT1 activity, 27 single-site mutants were generated and tested (Figure 2). Most of the amino acid residue substitutions had either positive or negative effects on BnaDGAT1 activity and neutral lipid accumulation. The results also indicated that the combination of two amino acid residue substitutions does not always affect BnaDGAT1 activity as expected. For example, L441P increased BnaDGAT1 performance, whereas either K110N or I287V resulted in decreased BnaDGAT1 performance (Figure 2). Thus, the combination of L441P with K110N or I287V may be expected to result in a lower enzyme activity than variant L441P. The results in Figure 1 and Table S1, however, show the following activity

ranking: L441P/I287V (D9) > L441P (B10 and C7) > L441P/K110N (D4). The most systematic way to determine possible synergies between amino acid residue substitutions leading to enhanced BnaDGAT1 performance would be to generate additional BnaDGAT1 variants with two or more favorable amino acid residue substitutions.

An in-depth study of five selected BnaDGAT1 variants suggested that the changes in yeast neutral lipid content might mainly involve altered enzyme activity (Figure 3). Moreover, site saturation mutagenesis at site 447 showed that different amino acid residue substitutions could result in substantial changes in BnaDGAT1 activity (Figure 4). Although I447F may not be the most effective DGAT1 variant (Figure 2), this experiment does show that substitution with conserved amino acid residues can be considered to explore the full potential of any DGAT1 variant. In addition, although the Nile red assay showed the effects of amino acid residue substitutions at position 447 on neutral lipid content, a more accurate quantification of TAG content by GC/FID (or GC/MS) would be a useful next step to explore the site saturation mutagenesis variants of position 447 in more detail. This analysis may also provide information on the effects of amino acid residue substitution on BnaDGAT1 selectivity.

Although the lack of a detailed three-dimensional structure makes it difficult to make a detailed structural interpretation of the effects of the various amino acid residue substitutions in the BnaDGAT1 variants, some interesting observations could be made by mapping the amino acid residue substitution sites onto a predicted topological model of BnaDGAT1 (Figure 5). It is known that different prediction algorithms vary in their prediction of membrane topology, particularly for membrane-bound *O*-acyl

transferases (MBOATs), including DGATs (Matevossian and Resh, 2015). As shown in Table S5, BnaDGAT1 was predicted to possess between eight and 10 TMDs in four prediction programs. The amino acid residues in each TMD slightly vary in different models, and the models predicted by TMHMM and SOSUI lack TMDs 5 and 8 and TMDs 5 and 6, respectively. The positions of most of the 81 amino acid residue substitutions in different TMDs were similar in all four models, except the ones on TMDs 5, 6 and 8, which have 1, 3 and 1 amino acid residue substitution sites, respectively. Here, we chose one model for further analysis (Figure 5). BnaDGAT1 has several putative substrate binding sites and active sites that mainly reside in the loops right before and after the first predicted TMD and the loops between the fourth and eighth predicted TMD (Weselake *et al.*, 2000; Jako *et al.*, 2001; Daniel *et al.*, 2004; Xu *et al.*, 2008; Liu *et al.*, 2012; Lopes *et al.*, 2014, 2015). The majority of the identified amino acid residue substitutions (72 of 81, 89%) identified via directed evolution, however, are located outside of the putative substrate binding and active sites (Figure 5). Directed evolution was used here as an efficient method to identify performance-enhanced BnaDGAT1 variants without considering the predicted active sites. The results indicated that these amino acids might be indirectly involved in the enzyme catalysis, and/or that the current model showing TMD sections, putative active sites and putative substrate binding sites might need to be improved. It is also noted that several amino acid residue substitutions resulting in BnaDGAT1 variants with increased performance are found within the hydrophilic N-terminal domain. This segment of BnaDGAT1 was previously found to bind acyl-CoA at a putative allosteric site, suggesting a possible role of this domain in enzyme performance (Weselake *et al.*, 2006). The current results suggest certain amino acid residue substitutions of the regulatory domain of BnaDGAT1 might modulate allostery so as to increase enzyme activity. In addition, some of these amino acid residue substitutions may have affected post-translational processing of the variants. As predicted by NETPHOSK, three sites (S54, S112 and Y386) from the 27 single-site variants contain the targets of protein kinase, and S54 and Y386 are the putative phosphorylation sites in BnaDGAT1 (Blom *et al.*, 2004). Similar to the enzyme activity change caused by modulating the phosphorylation state in other DGATs (Xu *et al.*, 2008; Liu *et al.*, 2012; Yu *et al.*, 2015), the amino acid residue substitution, S54T or Y386F, might affect post-translational processes and thus enhance BnaDGAT1 performance.

Some conserved residues of BnaDGAT1 are too essential to be modified, and thus might not be identified via directed evolution. For instance, H428 is highly conserved in the MBOAT family (Hofmann, 2000) but was not identified in this study (Figure 1). In the directed-evolution approach, BnaDGAT1 variants with increased performance

over the native enzyme are screened (Figure 1). Amino acid residue substitutions in the vicinity of the H residue may result in lower or lost activity, and are thus eliminated in the screening process. Moreover, it was demonstrated that F469 in maize DGAT1 is associated with enhanced TAG accumulation (Zheng *et al.*, 2008). Substitution of the equivalent amino acid residue (F477) in BnaDGAT1 was identified by directed evolution, but this variant has a total of five amino acid residue substitutions (including F477L; Table S1). This phenylalanine is conserved in almost all plant DGAT1s (Figure S2), and may have an important role in plant DGAT1 activity. In future work, it would be interesting to explore F477 and its 19 other amino acid residue substitutions through site saturation mutagenesis in BnaDGAT1 and other plant DGAT1s.

The amino acid residue sites identified in BnaDGAT1 are valuable for the study of other plant DGAT1s. Among the 18 single-site variants with increased TAG content (except L493*), 16 sites are recognized as moderately or highly conserved sites. As for the amino acid residue modification sites with less conservation, the substitutions S54T, C286Y, G332A or F449L occur naturally in other plant DGATs. In nature, positive selection (Darwinian selection) is a mode of natural selection by which new advantageous genetic variants sweep a population (Nielsen *et al.*, 2007). As for a specific enzyme, positive selection can affect enzyme functional divergence (Yuan *et al.*, 2017). As the directed evolution approach used in this study is an artificial selection mimicking the positive selection, but aimed towards a user-defined purpose (high activity in this case), it is interesting to identify positively selected sites in plant DGAT1 and compare them with the amino acid residue substitution sites identified in our study. A total of 83 positively selected sites were identified, and 21 of them, mainly in the less conserved N-terminus region, were included in the 81 BnaDGAT1 mutation sites (Figure S2). Therefore, these amino acid residue sites might play important roles in plant DGAT1s in general, in terms of molecular evolution.

With the important function of DGAT in TAG biosynthesis, the BnaDGAT1 variants could contribute to meeting the global demand for vegetable oil. As shown in Figure 6, the introduction of BnaDGAT1-I447F or BnaDGAT1-L441P significantly increased TAG content in *N. benthamiana* leaves, compared with native BnaDGAT1. The set of amino acid residue modifications resulting in BnaDGAT1 variants with increased activity can potentially be used to improve DGAT1s in other plants. Indeed, 67% of these amino acid residue sites were conserved across plant DGAT1s. In addition, the BnaDGAT1 variants can also be directly used to increase oil production in yeast such as *S. cerevisiae* and *Yarrowia lipolytica* beyond what can be attained via the naturally occurring acyltransferases. As shown in Figure 4, variants of I447F were even effective in yeast strain SCY62 (wild-type parent strain of H1246) under conditions where

variants compete with endogenous TAG biosynthetic enzymes.

In conclusion, we have gained novel insights into structure function in BnaDGAT1 through directed evolution, site-saturation mutagenesis, *in vitro* enzyme activity assay, topological analysis, and transient expression of cDNAs encoding selected variants of the enzyme in *N. benthamiana*. Our results showed that numerous amino acid residue sites substantially affected DGAT1 activity. The majority of the sites identified via directed evolution are located outside of the putative substrate binding and active sites. Moreover, the amino acid residue substitutions resulting in enhanced DGAT1 activity were predominantly polar. In addition, most of the identified modification sites in BnaDGAT1 were conserved in other plant DGAT1s, indicating their important functions in plant DGAT1 function in general. From the applied biotechnology perspective, selected BnaDGAT1 variants were significantly more effective in increasing the TAG content of vegetative tissue, compared with the native BnaDGAT1. In the future, it may be worthwhile to combine amino acid residue substitutions resulting in possible synergistic effects to enhance BnaDGAT1 activity even further.

EXPERIMENTAL PROCEDURES

Random, targeted and saturation mutagenesis of BnaDGAT1

BnaDGAT1-mutagenized libraries were generated by error-prone PCR using the GeneMorph II EZClone system (Stratagene, now Agilent, <http://www.agilent.com>; Siloto *et al.*, 2009a) using the cDNA encoding BnaC.DGAT1.a (Genbank# JN224473), which is the form of the enzyme recently purified by Caldo *et al.* (2015). Single amino acid residue substitutions and site-saturation mutagenesis at site 447 were introduced into the native BnaDGAT1 with the primers listed in Table S4 and degenerate primers using the QuikChange™ Site-Directed Mutagenesis Kit (Stratagene).

Heterologous expression of BnaDGAT1

Full-length *BnaDGAT1* cDNAs of native gene and mutants were cloned into the yeast expression vector pYES-Dest52 (ThermoFisher Scientific, <https://www.thermofisher.com>) under the control of the *GAL1* promoter (Siloto *et al.*, 2009a). To test the function of single amino acid residue substitution on DGAT1 activity, the encoding cDNA was inserted downstream of the *GAL1* promoter in the pYES2.1/V5-His-TOPO®TA yeast expression vector (ThermoFisher Scientific). *S. cerevisiae* strains were then transformed with both the experimental construct as well as the empty vector controls, as described in our previous papers (Siloto *et al.*, 2009a; Pan *et al.*, 2015). The *S. cerevisiae* strains used in this study were the quadruple knock-out strain H1246 (*MATa are1-D::HIS3, are2-D::LEU2, dga1-D::KanMX4* and *Iro1-D::TRP1 ADE2*), containing knock-outs of all four neutral lipid biosynthesis genes *DGA1*, *LRO1*, *ARE1* and *ARE2*, and the wild-type control strain SCY62 (*MATa ADE2*), kindly donated by Drs S. Stymne and U. Stahl (Sandager *et al.*, 2002). The recombinant yeast cells were first cultivated in liquid minimal medium containing 0.67% (w/v) yeast nitrogen base, 0.19% (w/v) SC-Ura and 2% (w/v) raffinose, and then grown

in minimal medium containing 2% (w/v) galactose and 1% (w/v) raffinose for the induction of gene expression (Pan *et al.*, 2015).

For heterologous expression in *N. benthamiana* leaves, WT and different *BnaDGAT1* variants were subcloned as *NotI-SpeI* fragments in a pORE04 binary vector containing a CaMV 35S promoter with duplicated enhancer region (Vanhercke *et al.*, 2013). A WT *BnaDGAT1* gene containing an N-terminal 6XHis tag was subcloned as a *Sall-SpeI* fragment into the same binary vector backbone. All constructs were transformed in *Agrobacterium tumefaciens* AGL1 and infiltrated into *N. benthamiana* leaves in the presence of the p19 viral suppressor protein, essentially as described by Vanhercke *et al.* (2013). Gene synthesis was performed by GeneArt (now ThermoFisher Scientific).

In vitro DGAT1 activity assay

Microsomal fractions were isolated from recombinant yeast cells for enzymatic assay, and the DGAT assay was performed with [14 C]-labeled acyl-CoAs as substrates (Caldo *et al.*, 2015). In brief, the enzyme assay was conducted in a reaction mixture (60 μ L) containing 200 mM HEPES-NaOH (pH 7.4), 3.2 mM MgCl₂, 333 μ M *sn*-1,2-diolein dispersed in 0.2% (v/v) Tween 20, 15 μ M [14 C] oleoyl-CoA (55 μ Ci μ mol⁻¹) (PerkinElmer, <http://www.perkinelmer.com>) and 2 μ g of microsomal protein. The reaction was initiated by the addition of microsomes containing recombinant DGAT1 variants and incubated at 30°C for 4 min with shaking before quenching with 10 μ L of 10% (w/v) SDS. The entire reaction mixture was applied onto a TLC plate (0.25-mm Silica gel; DC-Fertigplatten, Macherey-Nagel, <http://www.mn-net.com>), and the plate was developed with hexane/diethyl ether/acetic acid (80 : 20 : 1, v/v/v). After visualization by phosphor imaging (Typhoon Trio + GE Healthcare, <http://www.gehealthcare.com>), corresponding TAG spots were scraped and analyzed for radioactivity by an LS 6500 multipurpose scintillation counter (Beckman-Coulter, <http://www.beckmancoulter.com>).

Lipid analysis

Neutral lipid content in yeast cells was analyzed by Nile red fluorescence assay using either a Floureskan Ascent (ThermoFisher Scientific) or a Synergy H4 hybrid reader (Biotek Instrument Inc., <https://www.biotek.com>) or by GC/MS (Siloto *et al.*, 2009b; Chen *et al.*, 2012; Pan *et al.*, 2015). In brief, 100 μ L of yeast culture was incubated with 5 μ L of Nile red solution (0.1 mg mL⁻¹ in methanol) on a 96-well plate. The fluorescence was measured with excitation at 485 nm and emission at 538 nm, and the Nile red values were corrected for cell density based on OD₆₀₀ (Δ F/OD₆₀₀). TAG content and fatty acid composition of TAG-extracted yeast cells hosting various *BnaDGAT1* mutants were analyzed by GC/MS (Chen *et al.*, 2012). Total yeast lipids were extracted from lyophilized yeast cells, as described previously (Pan *et al.*, 2015). The isolated lipids were resolved on the TLC plates with the development solvent hexane/diethyl ether/acetic acid (80 : 20 : 1 v/v/v). TAG bands on the TLC plate were visualized by primuline staining and then were scraped and derivatized by incubation with 3N methanolic HCl for 1 h at 80°C. The fatty acid methyl esters were analyzed on an Agilent 6890N Gas Chromatograph (Agilent, <http://www.agilent.com>) with a 5975 inert XL Mass Selective Detector (Chen *et al.*, 2012).

In *N. benthamiana*, total lipids were extracted from leaf tissues using chloroform : methanol : 0.1 M KCl (2 : 1 : 1 v/v/v), as described by El Tahchy *et al.* (2017). TAG was fractionated by TLC (Silica gel 60; MERCK, <http://www.merck.com>) in hexane : diethylether : acetic acid (70 : 30 : 1 v/v/v), and visualized by spraying Primuline (5 mg/100 ml acetone : water, 80 : 20 v/v);

Sigma-Aldrich, <https://www.sigmaaldrich.com>) and exposing the plate to UV light. Fatty acid methyl esters (FAMES) of TAG were produced by incubating corresponding bands in 1 N methanolic HCl (Supelco, now Sigma-Aldrich) at 80°C for 2 h together with a known quantity of triheptadecanoin (Nu-Chek PREP, Inc., <http://www.nu-chekprep.com>) as an internal standard to quantify TAG. FAMES were analyzed by GC/FID (7890A GC; Agilent) equipped with a 30-m BPX70 column (0.25-mm inner diameter, 0.25-mm film thickness; SGE, Analytical Science, <http://www.sge.com>). Peaks were integrated with CHEMSTATION B.04.03 (Agilent).

Quantitative real-time PCR (qRT-PCR)

Yeast cells were homogenized in the presence of 0.5-mm glass beads by a bead beater (Biospec, <https://www.biospec.com>). RNA was extracted using the RNeasy Plant Mini Kit according to the manufacturer's instructions (Qiagen, <https://www.qiagen.com>). A 1- μ g portion of total RNA was used to synthesize first-strand cDNA in a 20- μ l reaction volume using an optimized blend of oligo-dT and random primers with the QuantiTect Reverse Transcription Kit (Qiagen). Quantitative RT-PCR assays were performed in triplicate using 1 μ l of a 1/20 dilution of each cDNA as template along with SYBR green PCR master mix on an ABI 7900HT Fast Real-Time PCR System (Applied Biosystems, now ThermoFisher Scientific) with *ACT1* cDNA (GenBank# NM_001179927.1) as the reference (Chen *et al.*, 2012). Thermal parameters for amplification were 95°C for 2 min, followed by 40 cycles of 95°C for 15 sec and 60°C for 1 min. The relative transcript abundance of the target gene in the individual seed sample was calculated using the comparative C_t method (Livak and Schmittgen, 2001). *BnaDGAT1* expression data consisting of mean values of the biological replicates were normalized with those of the *ACT1* internal control.

Western blotting

Isolated protein (10 μ g) was separated by 10% denaturing SDS-PAGE and then electrophoretically transferred to polyvinylidene difluoride membranes (Caldo *et al.*, 2015). Subsequently, the proteins were blocked with 2% Amersham ECL Prime Blocking Reagent before incubation with V5-HRP conjugated antibody (1 : 10 000). BnaDGAT1 content was visualized using ECL Advance Western Blotting Detection Kit (Amersham, now GE Healthcare), using a variable mode imager (Typhoon Trio+; GE Healthcare). The bands were semi-quantified using IMAGEJ (Schneider *et al.*, 2012).

Transmembrane domain prediction

A membrane protein topology prediction of BnaDGAT1 was obtained using the Protter visualization tool (<http://wlab.ethz.ch/protter>) following the protocol described by Omasits *et al.* (2014).

Statistical analysis

All experiments were repeated at least twice (n is the number of biological independent experiments). Data are shown as means \pm standard deviations (SDs) when $n \geq 3$, or mean \pm range when $n = 2$, unless otherwise stated. Statistical analysis was performed using the Student's t -test or one-way analysis of variance (ANOVA). Means were considered to significantly differ at $P < 0.05$.

ACKNOWLEDGEMENTS

The authors acknowledge support provided by Alberta Innovates Bio Solutions, Alberta Enterprise and Advanced Education, AVAC Ltd., the Canada Foundation for Innovation, the Canada Research Chairs Program, and the Natural Sciences and Engineering

Research Council of Canada (GC, RGPIN-2016-05926; RJW, RGPIN-2014-04585). Y.X. is a recipient of a scholarship from the China Scholarship Council and K.M.P.C. was a recipient of a University of Alberta Recruitment Scholarship and an Alberta Canola Producers Graduate Award in Canola Production Research.

CONFLICT OF INTEREST

The authors declare no conflict of interest.

SUPPORTING INFORMATION

Additional Supporting Information may be found in the online version of this article.

Figure S1. Amino residue acid substitutions in the 50 BnaDGAT1 variants.

Figure S2. Sequence alignment of DGAT1 from five typical plant species and location of positive selection sites.

Figure S3. Cell growth, gene expression and recombinant protein production of five BnaDGAT1 single-site mutants.

Table S1. Amino acid residue substitutions of the BnaDGAT1 variants.

Table S2. Fatty acid composition of triacylglycerol of yeast strains producing BnaDGAT1 variants.

Table S3. Twenty-two plant DGAT1s for sequence alignment.

Table S4. Primers used to generate 27 single-site mutants and for qRT-PCR.

Table S5. Predicted transmembrane domains (TMDs) in BnaDGAT1.

REFERENCES

- Blom, N., Sicheritz-Ponten, T., Gupta, R., Gammeltoft, S. and Brunak, S. (2004) Prediction of post-translational glycosylation and phosphorylation of proteins from the amino acid sequence. *Proteomics*, **4**, 1633–1649.
- Caldo, K.M.P., Greer, M.S., Chen, G., Lemieux, M.J. and Weselake, R.J. (2015) Purification and properties of recombinant *Brassica napus* diacylglycerol acyltransferase 1. *FEBS Lett.* **589**, 773–778.
- Carlsson, A.S., Yilmaz, J.L., Green, A.G., Stymne, S. and Hofvander, P. (2011) Replacing fossil oil with fresh oil- with what and for what? *Eur. J. Lipid Sci. Technol.* **113**, 812–831.
- Chen, G., Greer, M.S., Lager, I., Yilmaz, J.L., Mietkiewska, E., Carlsson, A.S., Stymne, S. and Weselake, R.J. (2012) Identification and characterization of an LCAT-like *Arabidopsis thaliana* gene encoding a novel phospholipase A. *FEBS Lett.* **586**, 373–377.
- Chen, G., Woodfield, H.K., Pan, X., Harwood, J.L. and Weselake, R.J. (2015) Acyl-trafficking during plant oil accumulation. *Lipids*, **50**, 1057–1068.
- Cheng, F., Zhu, L. and Schwaneberg, U. (2015) Directed evolution 2.0: improving and deciphering enzyme properties. *Chem. Commun.* **51**, 9760–9772.
- Daniel, J., Deb, C., Dubey, V.S., Sirakova, T.D., Abomoelak, B., Morbidoni, H.R. and Kolattukudy, P.E. (2004) Induction of a novel class of diacylglycerol acyltransferases and triacylglycerol accumulation in *Mycobacterium tuberculosis* as it goes into a dormancy-like state in culture. *J. Bacteriol.* **186**, 5017–5030.
- El Tahchy, A., Reynolds, K.B., Petrie, J.R., Singh, S.P. and Vanhercke, T. (2017) Thioesterase overexpression in *Nicotiana benthamiana* leaf increases the fatty acid flux into triacylglycerol. *FEBS Lett.* **591**, 448–456.
- Greer, M.S., Truksa, M., Deng, W., Lung, S.-C., Chen, G. and Weselake, R.J. (2015) Engineering increased triacylglycerol accumulation in *Saccharomyces cerevisiae* using a modified type 1 plant diacylglycerol acyltransferase. *Appl. Microbiol. Biotechnol.* **99**, 2243–2253.
- Grisart, B., Coppeters, W., Farnir, F. *et al.* (2002) Positional candidate cloning of a QTL in dairy cattle: identification of a missense mutation in the bovine *DGAT1* gene with major effect on milk yield and composition. *Genome Res.* **12**, 222–231.

- Hofmann, K. (2000) A superfamily of membrane-bound O-acyltransferases with implications for wnt signaling. *Trends Biochem. Sci.* **25**, 111–112.
- Jako, C., Kumar, A., Wei, Y.D., Zou, J.T., Barton, D.L., Giblin, E.M., Covello, P.S. and Taylor, D.C. (2001) Seed-specific over-expression of an Arabidopsis cDNA encoding a diacylglycerol acyltransferase enhances seed oil content and seed weight. *Plant Physiol.* **126**, 861–874.
- Liu, Q., Siloto, R.M.P., Lehner, R., Stone, S.J. and Weselake, R.J. (2012) Acyl-CoA:diacylglycerol acyltransferase: molecular biology, biochemistry and biotechnology. *Prog. Lipid Res.* **51**, 350–377.
- Livak, K.J. and Schmittgen, T.D. (2001) Analysis of relative gene expression data using real-time quantitative PCR and the 2(-Delta Delta C(T)) Method. *Methods*, **25**, 402–408.
- Lopes, J.L., Nobre, T.M., Cilli, E.M., Beltrami, L.M., Araujo, A.P. and Wallace, B.A. (2014) Deconstructing the DGAT1 enzyme: binding sites and substrate interactions. *Biochim. Biophys. Acta*, **1838**, 3145–3152.
- Lopes, J.L., Beltrami, L.M., Wallace, B.A. and Araujo, A.P. (2015) Deconstructing the DGAT1 enzyme: membrane interactions at substrate binding sites. *PLoS ONE*, **10**, e0118407.
- Matevossian, A. and Resh, M.D. (2015) Membrane topology of hedgehog acyltransferase. *J. Biol. Chem.* **290**, 2235–2243.
- Nielsen, R., Hellmann, I., Hubisz, M., Bustamante, C. and Clark, A.G. (2007) Recent and ongoing selection in the human genome. *Nat. Rev. Genet.* **8**, 857–868.
- Nykiforuk, C.L., Furukawa-Stoffer, T.L., Huff, P.W., Sarna, M., Laroche, A., Moloney, M.M. and Weselake, R.J. (2002) Characterization of cDNAs encoding diacylglycerol acyltransferase from cultures of *Brassica napus* and sucrose-mediated induction of enzyme biosynthesis. *Biochim. Biophys. Acta*, **1580**, 95–109.
- Omasits, U., Ahrens, C.H., Muller, S. and Wollscheid, B. (2014) Protter: interactive protein feature visualization and integration with experimental proteomic data. *Bioinformatics*, **30**, 884–886.
- Packer, M.S. and Liu, D.R. (2015) Methods for the directed evolution of proteins. *Nat. Rev. Genet.* **16**, 379–394.
- Pan, X., Chen, G., Kazachkov, M., Greer, M.S., Caldo, K.M.P., Zou, J.T. and Weselake, R.J. (2015) *In vivo* and *in vitro* evidence for biochemical coupling of reactions catalyzed by lysophosphatidylcholine acyltransferase and diacylglycerol acyltransferase. *J. Biol. Chem.* **290**, 18068–18078.
- Roesler, K., Shen, B., Bermudez, E. *et al.* (2016) An improved variant of soybean type 1 diacylglycerol acyltransferase increases the oil content and decreases the soluble carbohydrate content of soybeans. *Plant Physiol.* **171**, 878–893.
- Sandager, L., Gustavsson, M.H., Stahl, U., Dahlqvist, A., Wiberg, E., Banas, A., Lenman, M., Ronne, H. and Stymne, S. (2002) Storage lipid synthesis is non-essential in yeast. *J. Biol. Chem.* **277**, 6478–6482.
- Schneider, C.A., Rasband, W.S. and Eliceiri, K.W. (2012) NIH Image to ImageJ: 25 years of image analysis. *Nat. Meth.* **9**, 671–675.
- Siloto, R.M.P., Truksa, M., Brownfield, D., Good, A.G. and Weselake, R.J. (2009a) Directed evolution of acyl-CoA:diacylglycerol acyltransferase: development and characterization of *Brassica napus* DGAT1 mutagenized libraries. *Plant Physiol. Biochem.* **47**, 456–461.
- Siloto, R.M.P., Truksa, M., He, X.H., McKeon, T. and Weselake, R.J. (2009b) Simple methods to detect triacylglycerol biosynthesis in a yeast-based recombinant system. *Lipids*, **44**, 963–973.
- Vanhercke, T., El Tahchy, A., Shrestha, P., Zhou, X.R., Singh, S.P. and Petrie, J.R. (2013) Synergistic effect of *WRI1* and *DGAT1* coexpression on triacylglycerol biosynthesis in plants. *FEBS Lett.* **587**, 364–369.
- Vanhercke, T., Divi, U.K., El Tahchy, A. *et al.* (2017) Step changes in leaf oil accumulation via iterative metabolic engineering. *Metab. Eng.* **39**, 237–246.
- Weselake, R.J. (2005) Storage lipids. In *Plant lipids: biology, utilisation and manipulation* (Murphy, D.J., ed). Publishing: Blackwell, pp. 162–225.
- Weselake, R.J. (2016) Engineering oil accumulation in vegetative tissue. In *Industrial Oil Crops* (McKeon, T.A., Hayes, D.G., Hildebrand, D.F. and Weselake, R.J. eds). Amsterdam: Academic Press, and Champaign-Urbana, IL: AOCS Press, pp. 413–434.
- Weselake, R.J., Nykiforuk, C.L., Laroche, A., Patterson, N.A., Wiehler, W.B., Szarka, S.J., Moloney, M.M., Tari, L.W. and Derekh, U. (2000) Expression and properties of diacylglycerol acyltransferase from cell-suspension cultures of oilseed rape. *Biochem. Soc. Trans.* **28**, 684–686.
- Weselake, R.J., Madhavji, M., Szarka, S.J. *et al.* (2006) Acyl-CoA-binding and self-associating properties of a recombinant 13.3 kDa N-terminal fragment of diacylglycerol acyltransferase-1 from oilseed rape. *BMC Biochem.* **7**, 24.
- Weselake, R.J., Shah, S., Tang, M.G. *et al.* (2008) Metabolic control analysis is helpful for informed genetic manipulation of oilseed rape (*Brassica napus*) to increase seed oil content. *J. Exp. Bot.* **59**, 3543–3549.
- Winter, A., Kramer, W., Werner, F.A., Kollers, S., Kata, S., Durstewitz, G., Buitkamp, J., Womack, J.E., Thaller, G. and Fries, R. (2002) Association of a lysine-232/alanine polymorphism in a bovine gene encoding acyl-CoA:diacylglycerol acyltransferase (DGAT1) with variation at a quantitative trait locus for milk fat content. *Proc. Natl Acad. Sci. USA*, **99**, 9300–9305.
- Xu, J.Y., Francis, T., Mietkiewska, E., Giblin, E.M., Barton, D.L., Zhang, Y., Zhang, M. and Taylor, D.C. (2008) Cloning and characterization of an acyl-CoA-dependent diacylglycerol acyltransferase 1 (DGAT1) gene from *Tropaeolum majus*, and a study of the functional motifs of the DGAT protein using site-directed mutagenesis to modify enzyme activity and oil content. *Plant Biotech. J.* **6**, 799–818.
- Yu, J., Li, Y., Zou, F., Xu, S. and Liu, P. (2015) Phosphorylation and function of DGAT1 in skeletal muscle cells. *Biophys. Rep.* **1**, 41–50.
- Yuan, H., Wu, J., Wang, X., Chen, J., Zhong, Y., Huang, Q. and Nan, P. (2017) Computational identification of amino-acid mutations that further improve the activity of a chalcone-flavonone isomerase from *Glycine max*. *Front. Plant Sci.* **8**, 248.
- Zale, J., Jung, J.H., Kim, J.Y. *et al.* (2016) Metabolic engineering of sugarcane to accumulate energy-dense triacylglycerols in vegetative biomass. *Plant Biotech. J.* **14**, 661–669.
- Zheng, P., Allen, W.B., Roesler, K. *et al.* (2008) A phenylalanine in DGAT is a key determinant of oil content and composition in maize. *Nat. Genet.* **40**, 367–372.